

Fabrication and characterization of $\text{YBa}_2\text{Cu}_3\text{O}_7$ step-edge junction arrays

W. Reuter, M. Siegel, K. Herrmann, J. Schubert, W. Zander, and A. I. Braginski
*Institut für Schicht- und Ionentechnik, Forschungszentrum Jülich (KFA), P.O. Box 1913,
D-W 5170 Jülich, Germany*

P. Müller
Walther-Meißner-Institut, Walther-Meißner-Strasse 8, D-W 8046 Garching, Germany

(Received 11 November 1992; accepted for publication 18 February 1993)

We investigated one-dimensional arrays with up to 600 step-edge Josephson junctions (SEJ) fabricated by pulsed laser deposition of $\text{YBa}_2\text{Cu}_3\text{O}_7$ (YBCO) films on steep steps in epitaxial LaAlO_3 substrates. The steps were prepared by Ar-ion milling and the YBCO thin films were patterned either by Ar-ion milling or by an inhibit process. The current-voltage (I - V) characteristics and the Josephson emission of a single SEJ show that it consists of two resistively shunted-junction-type (RSJ) weak links in series which have different critical currents, I_{C1} and I_{C2} . The I - V characteristics of our arrays were also close to the RSJ-model. The number of series-connected weak links deduced from the I - V curves was usually higher than the number of steps. Histograms of the individual weak link I_C s showed two peaks at I_{C1} and I_{C2} . The I_C spread was about $\pm 20\%$ to $\pm 40\%$ of these two values. Radiation from arrays was detected and an evidence of phase locking in Josephson junction clusters obtained.

It has been shown that microbridges patterned from epitaxial $\text{YBa}_2\text{Cu}_3\text{O}_7$ (YBCO) films, which were deposited across steep steps in SrTiO_3 and LaAlO_3 substrates, are functioning as Josephson junctions.^{1,2} The static current-voltage (I - V) characteristics of such a step-edge junction (SEJ) indicate that it consists of two weak links in series, consistent with the existence of two grain boundaries located at the lower and upper edge of a step.³ The I - V characteristics of a single weak link are close to the resistively shunted junction (RSJ) model up to 85 K. Step-edge junctions have thus far been used in rf and dc superconducting quantum interference devices (SQUIDs).^{4,5} However, the performance of step-edge junctions is sufficiently high for a study of many other types of devices which have been previously investigated using thin films of low temperature superconductors (LTS). One interesting application are Josephson junction arrays used as tunable microwave oscillators. Considerable theoretical and experimental research has been done on LTS series array oscillators^{6,7} and investigations of two-dimensional arrays were also reported recently.⁸

We report here on the electrical properties of one-dimensional (series) step-edge YBCO Josephson junction arrays. The motivation of our work was to determine the spread of critical currents in the junctions and to detect Josephson radiation from the arrays. We also present some single SEJ data as a background reference.

Single SEJs and arrays were fabricated from pulsed-laser deposited YBCO films on $10 \times 10 \text{ mm}^2$ LaAlO_3 substrates. We used the fabrication process analogous to that developed for single SEJs and based on Ar-ion milling of YBCO films.² We also used an inhibit process⁹ to avoid degradation of the SEJ during the Ar-ion milling and the standard photolithographic processing. The steep steps in the LaAlO_3 substrates were fabricated by Ar-ion milling through photolithographic Nb masks. The step height was typically 300 nm while the thickness of the YBCO films was 200 nm. The SEJs were obtained by patterning 2- and

5- μm -wide microbridges positioned across the steps. After the fabrication process, the devices were annealed in an oxygen microwave plasma to increase the critical currents. The ohmic contacts to the arrays were made by ultrasonic bonding of Al wires on the Au contact pads which were evaporated on the YBCO film and lift-off patterned. Prior to the evaporation, the surface of the YBCO film was ion milled for some tens of seconds to obtain a satisfactory adhesion of the Au film. This removed the degraded film surface. The critical temperatures of the film and the SEJs were 90 and 85 K, respectively. The critical current density of the YBCO films without the SEJs was about $3\text{--}5 \times 10^6 \text{ A/cm}^2$ at 77 K.

The measurements of the I - V characteristics were performed with a low noise differential preamplifier connected to an I - V measurement system which contains an analog sweep generator controlling a current source and postamplifiers with active filters. The first derivative versus current was measured using a lock-in amplifier. The bias current and the voltage signal lines were filtered to avoid feeding the high frequency spurious signals to the arrays. The output signals were fed into a computer via an A/D converter.

Josephson emission into open space was measured at a frequency of 11–13 GHz. For the emission experiments the sample was mounted inside a horn at the end of an X-band waveguide. The signal was preamplified and mixed down with a local oscillator operating at 10–11 GHz. The intermediate frequency signal was monitored by a tuned vhf receiver at a fixed frequency and variable bias voltage. The bandwidth of the receiver was either 3 or 30 MHz.

The I - V characteristics of SEJs were shown and discussed in Ref. 3. The first derivative $\partial V / \partial I(I)$ shows two peaks. The first peak corresponds to the usual transition to the resistive state of a weak link above its critical current I_{C1} . The second, corresponding to a higher critical current value, I_{C2} , is attributed to a second weak link switching to the resistive state. The current-voltage characteristics of a

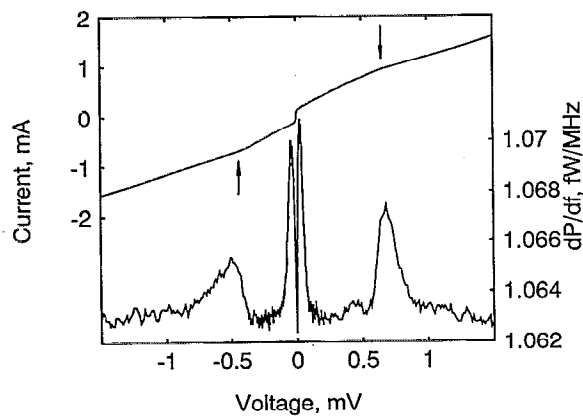


FIG. 1. The I - V characteristic (upper curve) of a SEJ and the corresponding spectral power density (lower curve) of microwave emission detected with a receiver at 12.7 GHz and 3 MHz bandwidth at 63 K.

SEJ biased well below the second critical current is close to the RSJ model. It was found that the I - V characteristics of SEJs with a width larger than the Josephson penetration depth exhibit a larger excess current than those of a narrow junction.³ The $I_C(H)$ characteristics determined for the two critical currents suggest that each of the two weak links in the SEJ can be represented by some parallel filamentary current paths.

We have studied the Josephson emission of single SEJs. That study will be reported separately.¹⁰ From that work, we reproduce data of Fig. 1 which show the I - V characteristic of a junction and the corresponding dependence of the emitted power spectral density dP/df vs bias voltage at 12.7 GHz and 63 K. The power density shows two peaks at bias voltages correlated with the two critical currents, I_{C1} and I_{C2} . The bias voltage of the first emission peak corresponds, exactly, to the Josephson relation $V = (h/2e)f$. The bias voltage at the second emission peak is correlated with the voltage where I_{C2} and a change in the normal resistance of the SEJ occur. An arrow in the I - V curve of Fig. 1 indicates this voltage drop on the already resistive first weak link. Subtracting it from the voltage of the second emission peak also gives a bias value expected from the Josephson voltage-frequency relation. The width of each emission peak is directly proportional to the Josephson emission linewidth, Δf . The asymmetry of both curves of Fig. 1 is caused by the flux trapped in the junction. The second emission peak shows unambiguously that a SEJ consists of a series connection of two weak links formed, presumably, at the upper and lower grain boundary present at steep steps in epitaxial substrates. After correcting for the load resistivity, the larger linewidth Δf of the second peak is consistent with the larger differential resistance R_d , according to the theoretical prediction: $\Delta f \propto R_d^2$. A detailed study of the SEJ linewidth determined by indirect and direct measurements is presented separately.^{10,11}

Using series arrays containing up to 600 step-edge junctions, we have studied the spread of the critical currents of the SEJs. The dimensions of the largest, 600 SEJ array were $150 \times 600 \mu\text{m}^2$ with a $5 \mu\text{m}$ distance between

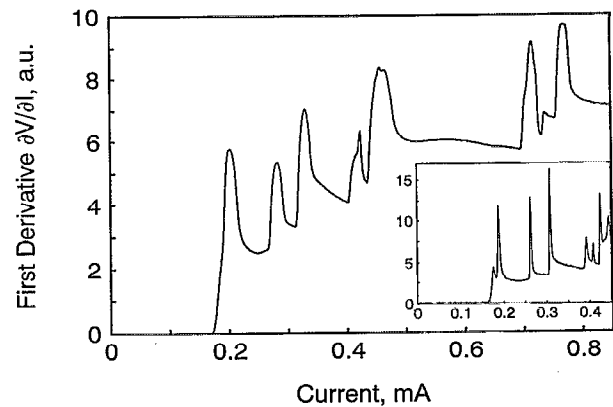


FIG. 2. First derivative $\partial V/\partial I$ vs current in a 10 SEJs series array at 4.2 K. The inset shows the same data over a narrower current range.

the adjacent SEJs. The $I_C R_N$ product of this array was found to be 450 mV with a normal resistance of 380Ω . The normal resistance of this and all other characterized arrays was determined by suppressing the critical current with microwave radiation. Most of the measured arrays were superconducting up to 81 K. We have determined the distribution function of the critical currents in the arrays by measuring the first derivative, $\partial V/\partial I(I)$ vs I . In Fig. 2, we show the $\partial V/\partial I(I)$ characteristic of a series array of 10 SEJs at 4.2 K. Data for such a short array are chosen for the clarity of presentation. Each of the multiple peaks seen in the characteristic corresponds to a critical current of at least one weak link. Peaks corresponding to identical and very similar I_C s are superposed so that a high current resolution is essential in these measurements. Insert in Fig. 2 shows the data over a narrower current range where additional peaks are resolved which cannot be seen in the curve covering a wider current range. The total number of resolved peaks exceed that of steps, consistent with the existence of two weak links at each step, i.e., in each SEJ. For large currents, not shown in Fig. 2, the average differential resistance reaches a maximum and then turns to lower values which is expected for a RSJ-like behavior. We have determined histograms of critical currents in five larger arrays, consisting of 30 or 100 SEJs each by counting the number of weak links switching into the resistive state in narrow bias current ranges. A representative example of an array of 30 SEJs is shown in Fig. 3. The distribution functions at 4.2 and 77 K exhibit two peaks at $I_{C1}(T)$ and $I_{C2}(T)$. The critical current is normalized to the value at the minimum between the two peaks, $I_{\min} = 4.2$ mA at 4.2 K and $I_{\min} = 0.4$ mA at 77 K. At 4.2 K, 32 peaks were counted while at 77 K only 12 could be identified unambiguously. The halfwidth spread (measured at $\frac{1}{2}$ of the maximum value) of the critical currents is about $I_{C1} \pm 20\%$ and $I_{C2} \pm 30\%$ at 4.2 K. The larger spread of the critical currents at 77 K is the likely consequence of somewhat different critical temperatures of the different weak links. We believed that the two peaks in the distribution function correspond to the two different weak links in each single SEJ. This belief was justified by the presence of similarly spaced two peaks in all recorded distributions. How-

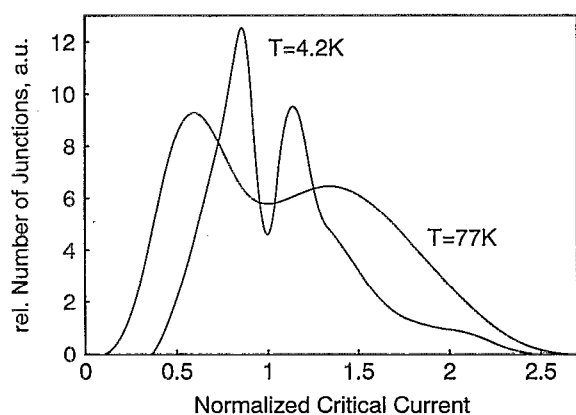


FIG. 3. Distribution functions of the critical currents at 4.2 and 77 K for a series connection of 30 SEJs. The current is normalized to I_{\min} ; $I_{\min}(4.2\text{ K})=4.2\text{ mA}$ and $I_{\min}(77\text{ K})=0.4\text{ mA}$.

ever, an alternative explanation has emerged from current, unpublished, low-temperature scanning electron microscopy measurements of spatial I_C distribution¹³ in our parallel arrays which are not discussed here. Identified were two I_C ranges attributed to two groups of SEJs located on opposite steps in the substrate. Such a spatial distribution could result from the atomic flux anisotropy during the film deposition. We don't know yet which explanation applies to the series-arrays discussed here.

Typically, the SEJs on LaAlO_3 substrates are highly damped, i.e., the McCumber parameter β_C is small. Using the RSJ model, we simulated an I - V curve of a series connection of 100 SEJ at 4.2 K by assuming $\beta_C=0$ and either a one- or two-peak Gaussian distribution function of the critical currents. The critical currents I_{C1} , I_{C2} , the average junction resistance and the halfwidth spreads were used as variable fitting parameters permitting to fit the simulation to the experimental I - V characteristic of a 100 SEJs array having a total resistance of 75 Ω . A one-peak distribution did not permit a reasonable fit. In contrast, a two-peak function yielded an excellent fit.

We could detect Josephson emission in all characterized arrays. Figure 4 shows the I - V characteristic and the detected microwave power spectral density of an array of 100 SEJs measured at 4.2 K. A major emission peak at a low bias and several smaller peaks at higher bias voltages can be seen. The I - V characteristic exhibits current upturns which cannot be explained by a model of series connected weak links. Such upturns are a typical signature of spontaneous phase locking of some of the weak links¹² and they are clearly correlated with the occurrence of emission peaks. The maximum spectral power density in the open-space measurement without matching is not representative of the emitted power. However, it should be noted that the peak values in the arrays have been up to an order of magnitude higher than in single junctions, i.e., about 5–10

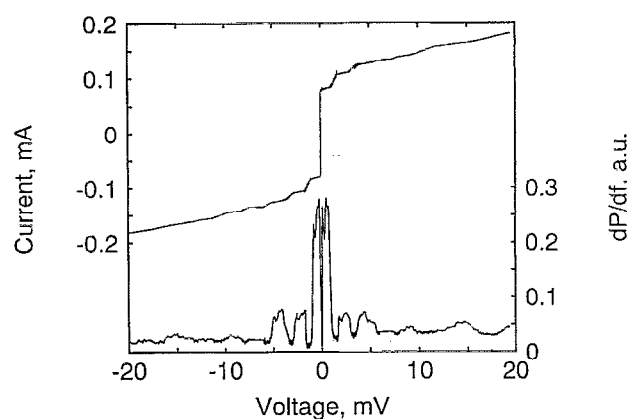


FIG. 4. A I - V characteristic (upper curve) of a series array of 100 SEJs and the emitted spectral power density (lower curve) detected with a receiver at 11.4 GHz and 30 MHz bandwidth at 4.2 K.

fW/MHz. In some arrays, sharp multiple emission peaks correlated with the single junctions critical currents were also observed. The emission from series arrays was observed over the temperature range between 4.2 and 77 K. In 10×10 two-dimensional arrays, which will be described separately, emission was detected up to 81 K.

To summarize, we have fabricated series arrays of up to 600 step-edge YBCO junctions and determined distributions of their critical currents. The I_C histograms show two peaks with critical current distribution of $\pm 20\%$ to $\pm 40\%$ around each peak. Josephson emission has been detected and evidence of phase locking of junction clusters in the array obtained. The results suggest the feasibility of fully synchronized arrays of high-temperature junctions having one narrow I_C distribution.

¹R. W. Simon, J. B. Bulman, J. F. Burch, S. B. Coons, K. P. Daly, W. D. Dozier, R. Hu, A. E. Lee, J. A. Luine, C. E. Platt, S. M. Schwarzbeck, M. S. Wire, and M. J. Zani, *IEEE Trans. Magn.* **27**, 3209 (1991).

²K. Herrmann, Y. Zhang, H.-M. Mück, J. Schubert, W. Zander, and A. I. Braginski, *Supercond. Sci. Technol.* **4**, 583 (1991).

³M. Siegel, K. Herrmann, C. Copetti, C. L. Jia, B. Kabius, J. Schubert, W. Zander, and A. I. Braginski, *IEEE Trans. Supercond.* **3** (1993).

⁴Y. Zhang, H.-M. Mück, K. Herrmann, J. Schubert, W. Zander, A. I. Braginski, and C. Heiden, *Appl. Phys. Lett.* **60**, 654 (1992).

⁵V. N. Glyantsev, M. Siegel, J. Schubert, W. Zander, U. Poppe, H. Soltner, A. I. Braginski, and C. Heiden, *IEEE Trans. Supercond.* **3** (1993).

⁶A. K. Jain, K. K. Likharev, J. E. Lukens, and J. E. Savageau, *Phys. Rep.* **109**, 309 (1984).

⁷J. Bindslev Hansen and P. E. Lindelof, *Rev. Mod. Phys.* **56**, 431 (1984).

⁸S. P. Benz and C. J. Burroughs, *Appl. Phys. Lett.* **58**, 2162 (1991).

⁹C. A. Copetti, U. Gassig, W. Zander, J. Schubert, and Ch. Buchal, *Appl. Phys. Lett.* **61**, 3041 (1992).

¹⁰P. Müller, K. Herrmann, M. Siegel, J. Schubert, W. Zander, and A. I. Braginski (unpublished).

¹¹Yu. Ya. Divin, A. V. Andreev, G. M. Fischer, J. Mygind, N. F. Peterson, K. Herrmann, V. N. Glyantsev, M. Siegel, and A. I. Braginski, *Appl. Phys. Lett.* (to be published).

¹²K. K. Likharev, *Dynamics of Josephson Junctions and Circuits* (Gordon and Breach, New York, 1986).

¹³K.-D. Huseman, R. Gross, and R. P. Hübner (unpublished).